Published in final edited form as:
Curr Protoc Cytom. 2012 April ; CHAPTER: Unit12.27. doi:10.1002/0471142956.cy1227s60.

Near-infrared Molecular Probes for In Vivo Imaging

Xuan Zhang, **Sharon Bloch**, **Walter Akers**, and **Samuel Achilefu***
Department of Radiology, Washington University School of Medicine, St. Louis, Missouri

Abstract

Cellular and tissue imaging in the near-infrared (NIR) wavelengths between 700 and 900 nm is advantageous for in vivo because of the low absorption of biological molecules in this region. This Unit presents protocols for small animal imaging using planar and fluorescence lifetime imaging techniques. Included is an overview of NIR fluorescence imaging of cells and small animals using NIR organic fluorophores, nanoparticles, and multimodal imaging probes. The development, advantages, and application of NIR fluorescent probes that have been used for in vivo imaging are also summarized. The use of NIR agents in conjunction with visible dyes and considerations in selecting imaging agents are discussed. We conclude with practical considerations for the use of these dyes in cell and small animal imaging applications.

Keywords

in vivo imaging; in vitro imaging; near-infrared fluorescent probe; confocal microscopy; fluorescence lifetime imaging

Optical imaging has been the mainstay of histology, bioassays, and microscopy for many decades because of the high spatial resolution and exceptional detection sensitivity of the method. Particularly, multiple-channel imaging distinguishes optical imaging from other imaging methods.(Hilderbrand and Weissleder, 20102010) Because of the large optical imaging window, typically between 400 and 1200 nm, it is possible to use multiple fluorescent probes in a single experiment without significant bleed through between the imaging channels. Therefore, multichannel imaging has great potential to facilitate the observation of multiple molecular targets in cells and tissue. For example, five distinct lymph node drainages were visualized in a single imaging session using dendrimers labeled with fluorophores of different colors.(Kobayashi, et al., 2007)

To be effective, many optical techniques require the use of designer molecular probes for detecting and tracking molecular processes or biomarkers of interest. Therefore, the development of new molecular probes has attracted the attention of researchers for many decades because of their diverse applications in chemistry, biology, and medicine.(Ballou, et al., 2005,Rao, et al., 2007,Sameiro and Goncalves, 2009) In recent years, optical imaging of molecular processes in living organisms has stimulated interest in the development of molecular probes for use in the near-infrared (NIR) region (700- 900 nm).(Achilefu, 2010,Escobedo, et al., 2010,He, et al., 2010,Hilderbrand and Weissleder, 2010) NIR molecular probes offer two major advantages over those that emit at visible wavelengths. First, biological tissues have lower absorption of NIR light than visible light.(Achilefu) This allows NIR light to penetrate deeper into tissue than light at visible wavelengths, thus enabling the assessment of information from deeper structures. Second, less autofluorescence is present at the NIR compared to visible wavelengths, enabling higher

Correspondence: Samuel Achilefu (achilefus@mir.wustl.edu).

signal-to-background ratios. Therefore, molecular probes that emit light in the NIR region are expected to be suitable for in vivo imaging. Recent research efforts have concentrated on developing and utilizing such NIR probes in biomedical imaging applications. In this chapter, the NIR fluorescent probes (exclusive of natural NIR proteins) that have been used for in vitro and in vivo imaging will be summarized. These include probes based on small-molecule organic fluorophores, nanoparticle-based probes and new multimodal imaging probes.

Basic Protocol 1: Planar NIR fluorescence imaging

Introductory paragraph

Whole Body Fluorescence Reflectance Imaging. Molecular probe localization within the body of small animals such as mice and rats can be visualized by fluorescence detection using the FRI system (Figure 1). Fluorescence imaging using FRI is high throughput, allowing imaging of multiple animals at one time and easy image analysis.

Materials—*Materials:*

Anesthesia (e.g. 2% isoflurane by nosecone or injectable such as 100 mg/kg ketamine, 10 mg/kg xylazine cocktail)

Fluorescent molecular probes (e.g. ProSense750, Perkin Elmer; IRDye® 800CW 2-DG, LiCor Biosciences)

Mice (15–25 g)

Light-tight imaging chamber with animal support systems (anesthesia, warming, positioning)

CCD-based preclinical fluorescence reflectance imaging (FRI) system (e.g. In-Vivo MS FX PRO, Carestream Health)

Broadband (Xenon) light source

Excitation bandpass filters

Emission bandpass filters

Digital camera, typically cooled to reduce electronic noise.

Software for acquisition and analysis of images (e.g. Molecular Imaging Software, Carestream Health)

Warming pad for recovery

Clear disposable Petri dish

Protocol—

1. Select excitation and emission optical filters to best detect fluorescent reporters used. For example, the detection of cypate fluorescence can be done with 760+/−10 nm excitation filter placed between broadband light source and subject and 830 +/− 15 nm wide-angle emission filter between subject and camera.

Emission filters are often larger (50 cm or greater) than those used for microscopy, so the center of bandwidth must be further from that of the excitation filter to prevent significant cross-talk.

2. Place anesthetized subject(s) on imaging platform within light-tight box. Position the region of interest (ROI) for best visualization by the camera.

   It is important to smooth any wrinkles in the area. It is also convenient to position small animals so that a reference area can be assessed for nonspecific uptake of molecular probes such as contralateral side. Correct placement can usually be assessed by "preview" function in the software using real-time brightfield imaging.

3. Acquire images using instrument software. Depending on the instrument software, selection of parameters to optimize image collection may be available.

   In our experience, acquisition time for 700 nm range fluorescence is 10–30 s and for 800–830 nm fluorescence is 30–60 s. Longer times are unlikely to significantly improve signal to background within the subject. If higher signal is needed, more of the imaging agent should be administered.

4. Remove subject(s) and place on warming pad until awake. Repeat with remaining subjects until all have been imaged for that time-point.

ROI analysis of image data—The fluorescence images are processed by using ROI analysis and calculation of the mean fluorescence intensity per tissue sample for each subject. Analysis can be performed using commercial software (e.g. Molecular Imaging Software, Carestreah Health) or open-source alternatives such as ImageJ (rsbweb.nih.gov/ij/). ROIs can be selected by hand or using automated functions in the software for comparison of mean intensity values for target and control tissues.

Basic Protocol 2: NIR fluorescence lifetime imaging

Materials

Anesthesia (e.g. 2% isoflurane by nosecone or injectable such as 100 mg/kg ketamine, 10 mg/kg xylazine cocktail)

Fluorescent molecular probes

Mice (15–25 g)

Preclinical Time-domain Diffuse Optical Imaging System (e.g. Optix MX2, Advanced Research Technologies, Montreal Canada)

670 nm and 780 nm laser excitation source

693 nm longpass filter and 850 +/−12 nm bandpass filter

Fast PMT with time-correlated single photon counting detection

Software for acquisition and analysis of images (e.g. Optiview, ART)

Warming pad for recovery

IMPORTANT NOTE: Experiments using live animals must first be reviewed and approved by your institution's Institutional Animal Care and Use Committee (IACUC) or according to your country's laws governing the use of animals in research.

Fluorescence lifetime imaging is a growing field in microscopy and now in deep tissue imaging. The fluorescence lifetime is the average time that a population of fluorophores remain in the excited state after light absorption (Lakowicz, 1988). Fluorescence lifetimes are unique characteristics of every fluorophore that are independent of dye concentration but can be sensitive to environmental conditions such as polarity, pH, temperature, protein binding and presence of ionic species. The Optix MX2 is a time-domain diffuse optical imaging system capable of measuring fluorescence intensity and fluorescence lifetime of NIR fluorescent reporters. A similar procedure is used for imaging of live animals as described for FRI.

1. Anesthetized animals are positioned on the heated imaging platform.

   The stage height must be adjusted.

2. The 2D scanning area can be set manually in the experiment set up wizard from a top view image.

3. The region selected will be raster-scanned for absorption at 780 nm and emission at 830 nm in 0.5 to 3 mm increments.

4. Laser power is automatically adjusted based on signal intensity detected during a brief pre-scan.

Data Analysis

Acquired data are analyzed with Optiview software provided by ART, Inc. (Montreal, Canada). Raw fluorescence data are smoothed by the program utilizing photo-information from the absorption scan. The software calculates fluorescence intensity by integrating the fluorescence decay curve. Fluorescence lifetime is calculated by fitting the tail of the decay curve, generally starting at 2–2.5 ns and ending at 6–11 ns. An initial fit is done manually for 2–3 pixels to visually assess the goodness of fit and check it against the chi-square of the fitting and the graphical error analysis tool. When the best time window is selected (chi-square near 1), fluorescence lifetime maps can be created for the whole scanned region using the software analysis tool. This step will require the best judgment of the investigator and comparison with in vitro measurements for the best results. ROI analysis can be performed to evaluate fluorescence intensity and lifetime in different areas of the subject.

COMMENTARY

Near-infrared Fluorescent Molecular Probes

The development of NIR molecular probes has become a major focus of research for optical imaging in recent years. In general, NIR imaging agents can be divided into probes based on small organic molecules and nanoparticles. The development of organic probes has been concentrated on obtaining desirable photophysical properties of the dyes, such as high quantum yields and/or long lifetimes, as well as improving their molecular targeting specificity. Despite the advantages of these small organic chromophores, as described below, the favorable characteristics of nanoparticle-based NIR probes has led to their inclusion in the library of materials available for optical imaging applications. Finally, the realization that a combination of imaging methods may be needed to provide comprehensive information about molecular events in tissue has led to the development of multimodal imaging agents. The development, advantages, and applications of these groups of NIR molecular imaging probes will be reviewed.

It should be mentioned that although autofluorescence is low in the NIR region, it is possible to image some structures without the use of a contrast agent. For example, the intensity of NIR autofluorescence in colonic cancer tissue is lower than in normal tissue. Further, when performed under polarization conditions and ratioed to NIR diffuse reflectance imaging, the differences between normal and cancer tissue are even more distinct.(Shao, et al.) Similarly, two-photon-excited autofluorescence generated with an NIR laser has been used to visualize elastin and collagen in pulmonary valves.(Schenke-Layland, et al., 2005,Schenke-Layland, et al., 2003) These miscellaneous aspects of NIR optical imaging will not be reviewed here. Interested readers are referred to pertinent literature on these topics.

NIR molecular probes based on small organic fluorophores

Currently, the commonly used NIR probes are based on small-molecule fluorophores, including polymethine cyanines, phthalocyanines, and squaraines.(Escobedo, et al.) Methods for the synthesis of these dyes are known and their spectral properties are tunable. Researchers have made tremendous efforts to modify the structures and properties of these dyes to meet diverse biological needs, including specific targeting of biomolecules of interest and reporting of molecular processes through fluorescence activation.

Cyanine dyes and their conjugates

The use of NIR fluorescent cyanine dyes for in vivo imaging started with the dye indocyanine green (ICG) (Fig. 2b) because it was readily available and had desirable NIR optical properties. Importantly, this is the only known NIR fluorescent dye approved by the US Food and Drug Administration (FDA) for monitoring cardiac output, hepatic function, and retinal angiography in humans.(Ogawa, et al., 2009) For optical imaging, various studies have shown that ICG accumulates in tumors through enhanced permeability and retention effects (EPR)(Kosaka, et al.,,Matsumura and Maeda, 1986) and it has also successfully been used to image tumors and lymph nodes.(Gurfinkel, et al., 2000,Owens, 1996) Many ICG derivatives or analogues have been designed and synthesized for different purposes, such as improving aqueous solubility or adding reactive functions for further bio-conjugation. For example, a hydrophilic glucamide-derivatized indocyanine (Fig. 2c) exhibited increased hydrophilicity and showed improved tumor-to-normal tissue contrast relative to ICG.(Licha, et al., 2000) Recently, a new class of cyanine fluorophores, PPCy dyes (Fig. 2d), has been synthesized via the reaction of diketopyrrolpyrrole with heteroarylacetonitriles.(Fischer, et al., 2009) These new cyanine dyes have exhibited interesting features for optical imaging, such as high quantum yields (>0.50), low photobleaching, and long fluorescence lifetimes (2.5 to 3.8 ns).(Berezin, et al., 2009,Fischer, et al., 2009) For these reasons, recent studies have explored PPCysas viable alternatives to NIR carbocyanine dyes for in vivo imaging. (Akers, et al., ,Akers, et al., ,Berezin, et al., 2009,Fischer, et al.)

Synthetic peptides offer several advantages as targeting agents, including high permeability to extravascular tissue, low immunogenicity, and ease of chemical modification. For example, studies have shown that the integrin $\alpha_v\beta_3$ receptor interacts with adhesion proteins such as fibronectin, vitronectin, collagen and fibrinogen in the extracellular matrix through an arginine-glycine-aspartic acid (RGD) peptide sequence. (Dijkgraaf, et al., 2009) Therefore, a number of cyanine-based NIR probes have been conjugated to RGD-containing peptides (Fig. 4a) and many of them exhibited selective uptake in tumors due to integrin $\alpha_v\beta_3$ receptor-mediated uptake of the conjugates.(Cheng, et al., 2005,Ye, et al., 2006).

Cyanine-based NIR fluorescent dyes have also been conjugated to antibodies, antibody fragments and antibody mimetics to achieve specific targeting to certain receptors. Representative receptors include the epidermal growth factor receptor (EGFR),(Ke, et al., 2003,Leung, 2004,Wang, et al., 2009) human epidermal growth factor receptor 2 (HER2)

(Ogawa, et al., 2009,Sampath, et al., 2007,Xiao, et al., 2009), insulin-like growth factor receptor (IGF-1R)(Chopra, 2004), vascular cell adhesion molecule-1(VCAM-1)(Leung, 2004), and the tumor-associated glycoprotein (TAG)-72.(Zou, et al., 2009) In addition, dye coupled small interfering RNAs (siRNAs) have been used as imaging agents (reviewed (Hong, et al.)) to report their delivery to cells, where the siRNAs inactivate gene expression. In fact, the use of NIR dyes coupled to siRNAs is an emerging and exciting field of research. (Sevick-Muraca, et al., 2002).

Although receptor-targeted molecular probes have been widely used in recent years, there are still some issues to be resolved, such as the occasional lag time between uptake in target tissue and clearance from non-target tissue. Therefore, alternative strategies to develop activatable NIR probes have become essential. In this case, instead of targeting specific cell-surface receptors, fluorescence is activated upon interaction with the intended molecular target after localization in a subcellular compartment. Examples include fluorescence enhancement by enzymatic cleavage of quenched probes or low pH environments such as lysosomes.(Hilderbrand, et al., 2008,Kobayashi and Choyke, 2011,Urano, et al., 2009)

Specific activation of fluorescence by diagnostic enzymes is one of the most common NIR optical imaging strategies with activatable probes. These molecular probes often contain two or more identical or different chromophores that are joined in close proximity to each other by an enzyme cleavable peptide linker. The probes initially have little or no fluorescence emission due to self-quenching effects (for identical chromophores) or fluorescence resonance energy transfer, FRET, mechanisms (for different chromophores). Cleavage of the peptide linker releases the fluorophores from each other, resulting in the restoration of strong fluorescence emission. The Weissleder group(Bremer, et al., 2001,Funovics, et al., 2003) pioneered this approach for in vivo imaging of tumor-associated protease activity in xenograft mouse models. In these series of studies, the NIR probe was bound to a graft copolymer of poly-L-lysine and methoxypolyethylene glycol, and tumoral NIR emission was generated through cleavage of the polymer chain by lysosomal proteases in tumor cells. To overcome the problem of reproducibility of labeling polymers with dyes, many research groups have explored the use of FRET mechanisms for monitoring the activities of target enzymes. Here, donor-acceptor dyes connected by a target enzyme cleavable peptide sequence are used. These NIR FRET probes have been used to demonstrate the activation of caspase-3 tumor cells and tumor bearing mice.(Komatsu, et al., 2006,Lee, et al., 2009,Linder, et al., ,Peng, et al., 2009,Zhang, et al., 2009)

New pH-sensitive NIR probes have recently been developed to assess intracellular pH changes in response to physiological and pathological processes and to monitor receptor-mediated trafficking of drugs and imaging agents in cells. Similar to enzyme activatable probes, the fluorescence of these probes is quenched until they encounter a low pH-environment, such as in the lysosomes. Under these conditions, protonation of an amine function incorporated into the dye chromophore produces significant spectral shift for ratiometric imaging or drastic changes in fluorescence intensity or lifetime of the probe. Toward this goal, several investigators have prepared pH-sensitive NIR dyes that emit light above 700 nm. One such example is a pH-sensitive NIR cyanine, H-ICG that has pK_a of 7.2, making it useful in the physiological range.(Zhang and Achilefu, 2005) Another example is the recent pH-sensitive cyanine dye (Fig. 4b) that responds to minor fluctuations in pH (6.70–7.90) *via* a photo-induced electron transfer mechanism. This molecular probe was successfully used to report the intracellular pH of HepG2 and HL-7702 cells in real time. (Tang, et al., 2009) Alternatively, a dual-ratiometric pH sensitive dye has been synthesized in which both the protonated and deprotonated forms are fluorescent. The deprotonated form has a very large Stokes shift, allowing for ratiometric measurement of pH.(Povrozin, et al., 2009) An interesting use of pH sensitive dyes is to deliver them to tumor cells and tissue.

This requires the functionalization of the probes for subsequent conjugation to protein, peptides, or other molecules of interest. Cooper *et al.*(Cooper, et al., 2002) successfully demonstrated the cell tracking of antibodies labeled with a pH-sensitive cyanine dye. More recently, Lee *et al.*(Lee, et al., 2011) synthesized and conjugated a new NIR pH-sensitive probe with cyclic RGD peptide to achieve specific targeting of the integrin $\alpha_v\beta_3$ dimeric protein which is overexpressed on proliferating tumor cells. Subsequent receptor-mediated endocytosis through the lysosomal pathway led to the protonation of the probe in the acidic cellular organelle, with the attendant fluorescence enhancement in tumor cells as well as tumor tissue in vivo.

The unique ability to manipulate the fluorescence properties of organic dyes with ease through astute design of the chromophore core has allowed the development of other molecular sensing mechanisms. For instance, reduction of carbocyanines with borohydride generates hydrocyanines (Fig. 3c) which are weakly fluorescent until oxidized. Using this molecular construct, Kundu *et al.*(Kundu, et al., 2009) demonstrated selective enhancement of hydrocyanines in vivo upon their oxidation by reactive oxygen species (ROS). Without doubt, many other elegant strategies to detect specific biomolecules or processes in the NIR region will become available in future as researchers become aware of unique biological problems that can be solved by activatable fluorescence probes.

Dyes based on other small organic fluorophores

Tetrapyrrole-based compounds, such as porphyrins, chlorins, benzochlorins, phthalocyanines, and expanded porphyrins, have been widely used as photodynamic therapy (PDT) agents.(Ochsner, 1997) However, they are also used for diagnostic purposes because of their significant fluorescence in both the visible and NIR regions. A variety of tetrapyrrole-based compounds, such as hematoporphyrin (HpD),(Dougherty, et al., 1976) meso-tetra-*m*-hydroxyphenylchlorin (*m*-THPC) (Fig. 4a),(Alian, et al., 1994) benzoporphyrin derivatives (BPD),(Andersson-Engels, et al., 1993) and sulfonated phthalocyanines,(Cubeddu, et al., 2000) derivatives of chlorin e6, have been used for combined fluorescence imaging and PDT capabilities. Another commonly used PDT procedure starts with the intravenous injection or topical application of 5-aminolevulinic acid, which converts to heme through the biosynthetic pathway.(Peng, et al., 1997) In the last step of the heme biosynthesis, iron is incorporated into the intermediate Protoporphyrin IX (PpIX). Although heme is not fluorescent, PpIX has similar NIR emission as other porphyrin-basd compounds. This has allowed for the use of PpIX fluorescence to detect and visualize tumors and other abnormal tissues.(Hewett, et al., 2001) More recently, PpIX was conjugated with cyclic RGDfK peptide, and the conjugate showed significant retention and accumulation in tumor tissue along with higher tumor to normal tissue ratios than the free PpIX in a mouse CaNT tumor model.(Conway, et al., 2008)

Squaraines, polymethine dyes with a zwitterionic structure, are one of the most important classes of dyes which can be used for imaging due to its narrow and intense absorption/emission bands in the NIR region. Squaraine dyes and their conjugates have been prepared and evaluated for various types of applications, including in vivo fluorescence lifetime and cellular imaging.(Arunkumar, et al., 2005,Arunkumar, et al., 2006) One of the problems with the use of squaraine dyes in aqueous media is the low stability of the compounds. To overcome this problem, the highly electrophilic squaraine chromophore was encapsulated in a macrocyclic structure (Fig. 4b), which further minimized self-aggregation.(Johnson, et al., 2007) The resulting squaraine rotaxane has been used to successfully detect *E. coli* and *S. aureus* bacteria in living mice. The fluorescence emission at sites of bacterial inoculation was about 100 times greater than the background signal from the reference tissue.

Other widely used fluorescent probes for biomedical applications are BODIPY (borondipyrromethane) dyes (Fig. 4c). Although most of these dyes have emission maxima in the visible region, several research groups have focused on developing new NIR BODIPY dyes by extending the π-bond chromophore conjugations.(Umezawa, et al., 2009,Umezawa, et al., 2008) For example, Zheng *et al.*(Zheng, et al., 2008) have prepared a series of conformationally restricted BODIPY dyes that exhibit increased fluorescence quantum yields with NIR emissions. The group successfully demonstrated the use of one- and two-photon fluorescence microscopy to image the uptake of these BODIPY dyes by HeLa cells.

Besides the small NIR organic fluorophores described above, other molecules have been designed to report molecular events in the NIR region. Although the majority of these agents are designed for imaging tumor cells, they are also used to image other diseases,(Meek, et al., 2008,Yang, et al., 2008) such as rheumatoid arthritis(Gompels, et al.) and Alzheimer's disease(Nesterov, et al., 2005) For example, Swager and coworkers(Nesterov, et al., 2005) have reported a series of push-pull-type NIR dyes (Fig.4d) that only emit fluorescence when bound to β-amyloid, a component of plaques in Alzheimer's disease. The researchers further identified one of the dyes binds to β-amyloid plaque in a living mouse brain with high sensitivity and specificity.

Nanoparticle-based NIR molecular probes

In recent years, many efforts have been made to develop novel NIR nanoparticles for in vivo molecular imaging to overcome some of the limitations of conventional NIR organic fluorophores, which includes poor hydrophilicity and photostability, as well as low fluorescence quantum yield. In this section, nanoparticle-based NIR probes (Fig. 5) that can be used for in vitro and in vivo imaging is briefly reviewed.(He, et al., 2010,He, et al., 2010,Xing, et al., 2009)

Quantum dots

Quantum Dots (QDs) are semiconductor nanocrystals, exhibiting interesting optical properties desirable for molecular imaging. These properties include narrow and tunable emission bands, high molar extinction coefficients, high fluorescence quantum yields, large effective Stokes shifts, and high resistance to photobleaching.(Gao, et al., 2010,Tavares, et al., 2011,Zheng, et al., 2007) They are composed of materials from the elements in the periodic groups of II–VI, III–V or IV–VI, Examples of such elements include cadmium telluride (Cd from group II and Te from group VI) and indium phosphamide (In from group III and P from group V). These nanoparticles generally range in size from 2 to 10 nm in diameter and contain approximately 200–10,000 atoms.(Smith, et al., 2008) Although visible light-emitting QDs dominated the initial biological applications of these materials, recent efforts have focused on developing stable NIR emitting QDs. In particular, QDs are attractive for a variety of applications because their luminescence can be easily tuned from the visible to the NIR wavelengths, depending on their size, chemical composition, and surface chemistry.

Two common synthetic routes, organic and aqueous synthesis, have been used for the synthesis of QDs.(Peng and Peng, 2001,Qian, et al., 2006) The organic synthesis method for the preparation of QDs is carried out by heating the appropriate organometallic precursors in organic solvents.(Peng and Peng, 2001) Although high quality and monodispersed QDs can be obtained from this method, the resulting QDs are usually very hydrophobic. Conversely, water-soluble QDs can be synthesized in aqueous solution by the hydrothermal method using thiols as stabilizing reagents.(Li, et al., 2005,Qian, et al., 2006) However, QDs prepared by the aqueous synthesis method suffer from poor crystallinity, low quantum yield, and long reaction times. Therefore, high-quality QDs are usually synthesized at high-

temperature in hydrophobic solvents using the organic synthesis method, and then transferred to the aqueous phase by replacing the hydrophobic surface coating with bifunctional ligands, such as mercaptoacetic acid and 11-mercaptoundecanoic acid.(Jin, et al., 2008,Smith, et al., 2008) These bifunctional ligands generally contain a thiol group that binds strongly to the QD surface and another group such as a carboxylic acid to serve as both water-solubilizing and reactive components for labeling various biomolecules with the QDs.

The attractive optical properties of Qds have facilitated their use in both cell microscopy and animal imaging. For example, Morgan *et al.*(Morgan, et al., 2005) reported the use the CdMnTe/Hg QD coated with bovine serum albumin (emitted at 770 nm) as an angiographic contrast agent. It was demonstrated that blood vessels on the order of 100 μm in diameter and located at a depth of several hundred microns could be visualized after injecting these NIR QDs either subcutaneously or intravenously into athymic mice. In another study, Kim *et al.*(Kim, et al., 2004) reported the utility of NIR QDs (CdTe/CdSe) for sentinel lymph node imaging in the mouse and pig models. In 2007, multicolor NIR imaging of lymphatic system was achieved by using two near infrared quantum dots with different emission spectra, which allow non-invasive and simultaneous visualization of two separate lymphatic flows draining the breast and the upper extremity.(Hama, et al., 2007)

To deliver the nanoparticles to specific tissues, the NIR QDs have been modified with targeting moieties on their surfaces. For example, when RGD peptide-labeled QD705 was used as an imaging agent in nude mice bearing subcutaneous U87MG human glioblastoma tumors, the tumor fluorescence reached a maximum at 6 h post-injection with very good contrast.(Cai, et al., 2006) Smith *et al.*(Smith, et al., 2008) directly observed and recorded the binding of nanoparticle conjugates (QD800-RGD) to newly formed/forming tumor blood vessels expressing $\alpha_v\beta_3$ integrin in living subjects using intravital microscopy with subcellular (approximately 0.5 micron) resolution. Another interesting application is the QD-mediated non-invasive imaging of growth factor receptors (e.g. epidermal growth factor receptor, EGFR important in cancer detection and therapy. To accomplish this goal, Diagaradjane *et al.*(Diagaradjane, et al., 2008) developed EGF-conjugated QD800 nanoprobes to image EGFR expression in human colon cancer xenografts. The EGF-QD progressively accumulated in tumors from 1 to 6 h post-injection while pure QD concentration gradually decreased in tumors over this time. At 24 h post injection, the tumor fluorescence decreased to near-baseline levels for both QD and EGF-QD. The measurable contrast enhancement of tumors after 4 h and the subsequent decrease in fluorescence at 24 h suggest the potential use of this nanoprobe for quantitative and longitudinal imaging of EGFR expression.

QDs can also emit light by other mechanisms. So *et al.*(So, et al., 2006,So, et al., 2006) recently reported the development of self-illuminating NIR QD conjugates (Fig.6). The conjugates were prepared by coupling QDs to a mutant of light-emitting proteins *Renilla reniformis* luciferase (Luc8). The QD luminescence is based on bioluminescence resonance energy transfers (BRET), which converts chemical energy into light. After adding the substrate coelenterazine, the protein Luc8 catalyzes the oxidation of coelenterazine and emits light with a peak at 480 nm. This energy then transfers to the QDs in close proximity, leading to the NIR emission. The resulting conjugate exhibited enhanced sensitivity in small animal imaging, with an in vivo signal-to-background ratio of more than 10^3 for 5 pmol of the conjugate. More recently, the same group further reported their new approach in self-illuminating QDs.(Ma, et al., 2010) Herein, Luc8 was used as a template to direct the synthesis of PbS QDs at ambient conditions to form a Luc8–PbS complex. This new type of QDs exhibited photoluminescence in the range of 800–1050 nm by BRET mechanism. Impressively, the Luc8 enzyme remained active within the Luc8–PbS complex.

All of the above demonstrates that QDs are excellent candidates for many biochemical imaging applications. However, there are concerns and limitations related to the use of QDs and their conjugates for in vivo imaging. For instance, potential toxicity of the constituents of QDs remains a real or perceived concern for long term use of these nanoprobes for biomedical applications. This concern is driven by the established acute and chronic toxicities of the heavy metals such as cadmium, tellurium and selenium, which are used in some QD preparation.(Hardman, 2006)

NIR dye-labeled nanoparticles

The nanoparticles described in this section are those incorporating small organic NIR dyes.(Santra, et al., 2005) These NIR dye-containing nanoparticles have a typical core-shell structure in which the core is an NIR organic dye and the shell is polymer or inorganic matrix-based particles. The high payload of NIR organic dyes are usually embedded inside the particles either noncovalently or covalently. For in vivo cancer imaging applications, NIR dye-containing nanoparticles are extremely attractive due to the following advantages. First, enhanced photostability can be achieved through the shell protection of the NIR dyes from outside quenching and other degrading factors. Second, improved solubility in aqueous media is obtained through the incorporation of hydrophilic shell materials. Third, enhanced fluorescence can be acquired via a high payload of dye molecules per nanoparticles. Lastly, it is easy and straightforward to conjugate biomolecules to the functional groups of the shells and to create multifunctional nanoparticles. NIR dye-containing nanoparticles, such as NIR dye-doped silica nanoparticles,(Santra, et al., 2001) calcium phosphate nanoparticles (CPNPs),(Dorozhkin and Epple, 2002) and organic nanoparticles,(Tosi, et al., 2011), have been explored as in vivo imaging probes.

Among the inorganic products used as matrix materials in dye-containing nanoparticles, amorphous silica appears to be an excellent choice because it is biocompatible and nontoxic. Furthermore, the surface hydroxyl groups on the silica shell can be chemically modified with amines, carboxyls, or thiols for further conjugation. These silica-based nanoparticles have been used for in vivo imaging. For example, Lee *et al.*(Lee, et al., 2009) reported the biodistribution study of ICG-doped mesoporous silica nanoparticles in rats, which demonstrated the nanoparticles have strong and stable fluorescence, and display prominent uptake in the liver. Another inorganic material, calcium phosphate (CP) is generally considered to be safe due to its presence throughout the body (e.g., bones, teeth). Altınoglu *et al.*(Altınoğlu, et al., 2008) designed and prepared PEGylated ICG-doped CPNPs and demonstrated that they accumulated in breast adenocarcinoma xenografts at 24 h after intravenous tail vein injection. In contrast, the fluorescence of free ICG in the tumor was relatively short because of its rapid clearance from the body. Ex vivo tissue imaging further demonstrated that detectable penetration and emission depths are seen with ICG-CPNPs at 3 cm in porcine muscle tissue compared to the weakly fluorescent free ICG at only 2 cm. These results support the potential of using ICG-doped CPNPs for early detection of solid tumors.

Besides the inorganic nanoparticles used as matrix materials, organic polymers have also been used to prepare NIR dye-containing nanoparticles. Tosi *et al.*(Tosi, et al., 2011) synthesized and administered poly-lactide-co-glycolide (PLGA) nanoparticles conjugated with near-infrared (NIR) probe (DY-675) and a simil-opioid glycopeptide (g7). The PLGA nanoparticle with g7 peptide has already proved to be a promising tool for achieving successful brain targeting after intravenous administration in rats.(Costantino, et al., 2005) Optical imaging clearly showed the localization of these novel polymer-based NPs in the brain, demonstrating that they were able to cross the blood-brain barrier.(Tosi, et al., 2011) In another study, NIR-emissive polymersomes (50 nm to 50 μm diameter polymer vesicles) were generated through self-assembly of amphiphilic diblock copolymers and conjugated

multi(porphyrin)-based NIR fluorophores. The study demonstrated that the fluorescence emanating from the probes was detectable through the dense tumor tissue of a live animal. (Ghoroghchian, et al., 2005)

Other nanosized NIR probes

In addition to QDs and NIR dye-containing nanoparticles, several other nanosized probes can be used as NIR fluorescence imaging agents. An important class of these materials is carbon nanotubes (CNTs). These nanoparticles can be classified as single-walled nanotubes (SWNTs) or multiwalled nanotubes (MWNTs). Current research with CNTs has primarily focused on their mechanical, thermal and electronic properties and their potential application in electronic devices. However, the optical properties of CNTs and their application in biomedical imaging were explored after the discovery of fluorescent semiconducting CNTs. SWNTs are promising NIR nanomaterials for optical imaging because of their unique features.(Liu, et al., 2009, O'Connell, et al., 2002) First, the emission of SWNT-based probes is primarily in the region of 1000–1400 nm, which is suitable for in vivo imaging. Second, a large Stokes shift often exists between the excitation and emission bands of SWNTs, which minimizes spectral bleed-through artifacts of the excitation light. Third, SWNTs possess a large surface area that facilitates the incorporation of large amounts of targeting ligands or drugs. Finally, SWNTs are highly photostable, which allows them to serve as NIR tracking probes for longitudinal measurements.

Another class of nanosized particles is derived from gold. Gold-based nanomaterials, such as nanoshperes, nanotubes, nanoshells, and nanorods, have been used as contrast agents for biological imaging of cancer in vivo because of their NIR surface plasmon bands.(Bakshi, et al., 2007, Zheng, et al., 2003) Small gold nanoclusters with sizes below 2 nm have drawn significant attention in recent years. These nanoclusters are composed of a small number of gold atoms, resulting in molecule-like characteristics that include discrete electronic states and size-dependent fluorescence.(Huang, et al., 2009) A variety of templates or ligands have been used to prepare gold nanoclusters with emissions in the visible region, including poly(amidoamine) dendrimer, mercaptoundecanoic acid and lipoic acid as nanoparticle. Recently, an environmentally friendly method was used to prepare NIR gold nanoclusters using bovine serum albumin (BSA) as a template.(Xie, et al., 2009) The development of bright, small-sized NIR gold nanoclusters and the stable optical features of these materials strongly suggest their potential use in cellular and biological imaging applications.

Ex-vivo biodistribution of probes can be performed using the simple method described in previous studies using a FRI system (Achilefu, et al., 2000, Bugaj, et al., 2001). After imaging, animals are humanely euthanized. Aliquots of blood and samples of all major organs (tumor, heart, kidney, lung, spleen, stomach, intestine, muscle, adrenals, pancreas, liver, skin and brain) are collected, washed with PBS, dabbed dry and weighed. The organs and a small sample of blood are placed in a clear Petri dish and placed on the imaging platform within the field of view of the camera. Images are acquired using the same optical filters and settings as for live animal imaging.

Diverse NIR molecular probes are available for use in biological imaging. Most researchers are interested in using these molecular probes at both cellular and tissue levels, which permits the translation of findings in cells to multicellular living organisms such as rodents and humans. In addition to the wide use of small-molecule organic fluorophores, nanoparticle-based probes offer alternative strategies for in vitro and in vivo imaging. Developments on the multimodal and/or multicolor probes open the door for exciting applications. Although tremendous efforts have been made towards developing new NIR probes, continued efforts to further improve the photophysical and biological properties of the new probes are still in progress.

Although small animal imaging systems are readily available in most research institutions, NIR confocal microscopy capability only became feasible a few years ago.(Achilefu, et al., 2005) Many factors led to this lag. First, most cell biology research focused on visible light, which also had the advantage of visualizing gross color changes with to the naked eye. Second, shorter wavelengths provide higher spatial resolution than longer wavelengths. Finally, most microscopes are equipped with detectors that are optimized for imaging in the visible region. However, a new generation of detectors is becoming available for NIR cellular imaging. We envisage that many researchers will incorporate these new detectors as part of their imaging platform in the future. Another emerging area is the use of lasers with long excitation wavelengths for multiphoton microscopy with NIR fluorophores. In contrast to the conventional multiphoton microscopy where NIR light is used to excite visible dyes, this all-NIR two photon microscopy approach harnesses the higher depth profiling capability of NIR light, as demonstrated by recent reports.(Murari, et al., 2011,Yazdanfar, et al., 2010) If the new all NIR multiphoton imaging method demonstrates significant improvement in depth profiling, the technology is anticipated to become an integral part of multiphoton microscopy in future.

Critical Parameters

How to choose a dye—Cyanine dyes (generic structure for carbocyanine dyes is shown in Fig. 2a) are the NIR dyes of choice for imaging molecular events in cells and tissues because they have exceptionally high extinction coefficients (>100,000 M^{-1} cm^{-1} for some carbocyanine dyes)(Ying and Branchaud) and fluorescence quantum yields (>0.8 for some pyrrolopyrrole cyanine (PPCy) dyes).(Fischer, et al., 2009) The combination of both high extinction coefficients and quantum efficiency generates bright fluorescent compounds, which in turn favors the use of small amounts of these probes to detect less abundant target biomolecules. The dyes have an odd number of carbons in a conjugated polymethine framework of heterocyclic rings, such as benzoxazole, benzothiazole, indolyl, 2-quinoline and 4-quinoline at the end of the polymethine chain.(Licha, 2002) Thus, the careful selection of polymethine chain length and the nature of the heterocyclic rings represent a viable strategy to generate cyanine dyes with desirable optical properties. Derivatives of the parent dyes can be functionalized with reactive groups such as amines and carboxylic acids for ease of conjugation to drugs or targeting groups for delivery to specific cellular compartments or tissue types.

Practical considerations for in vivo imaging

There are several areas that must be addressed in the design of in vivo molecular imaging studies. The choice of animal model is important in the final success of the experiment. For optical imaging, the resolution diminishes (?) with depth below the skin surface, particularly with FRI. Thus, it might be difficult to detect a small structure at depths >1 mm, while the same structure would be easily visible with direct exposure. For example, the pancreas and prostate are relatively small organs that exist near the axial center of the mouse body. They are also surrounded by clearance organs including the liver, intestines, kidneys and bladder, which will likely have high fluorescence during the first 24–48 hours post-injection of an imaging agent. Thus, a molecular probe with extremely high selectivity for these organs might not be detected by noninvasive imaging methods, or may be detected as a large fluorescence region due to scattering of the emitted photons as they penetrate to the skin surface. The most important parameter is acquisition time. Longer acquisition times result in greater signal detection relative to background noise from the instrument. For most commercial dyes, 1–2 nmol/25 g mouse produces adequate signal over 24 hrs. Pilot studies should be performed with new agents to optimize signal detection.

Practical considerations for imaging cells with a NIR confocal microscope

Several protocols published in this journal have addressed diverse techniques in microscopy and will not be reproduced here. The NIR fluorescence confocal microscope follows similar protocols as conventional systems, with the exception that the light source and detector system are optimized for NIR fluorescence imaging. In our laboratory, cells treated with NIR probes are imaged using a reconfigured Olympus FV 1000 confocal microscope. A 785 nm laser diode is used as the light source and a 817 +/− 25 nm bandpass filter acts to attenuate emitted light outside the NIR range. The microscope is also equipped with three lasers that excite in the visible region, allowing for imaging of multiple fluorophores in the same samples. Thus, subcellular localization of the NIR probes can be determined by co-staining the cells with commercially available dyes that label mitochondria, lysosomes, etc (Figure 7). Because the alignment of the NIR channel is slightly different from that of the other channels the images must be realigned when they are overlaid, but this is can be done easily with image processing software such as ImageJ. When comparing samples, it is important that all images be taken at the same settings, as increasing the laser power or voltage results in an increase in fluorescence intensity. To obtain accurate quantitation of relative fluorescence, the settings should be adjusted so that the highest fluorescence is below the saturation threshold for the system. Often it is necessary to image the samples at multiple settings as dyes which do not internalize as well might only be visualized at settings which will saturate the signal from better internalizing dyes. It is also important to choose probes that are both compatible with the microscope filters and do not have overlapping emissions or excitations, which would result in a probe fluorescing in more than one channel. Similarly, high concentration of a molecular probe can result in bleeding into another channel; consequently, it is important to optimize staining with each dye individually before labeling cells with multiple probes. Spectral overlap can also be minimized by selecting the microscope software setting for sequential imaging, that is with only one laser exciting the sample at a time, as opposed to imaging the channels simultaneously.

Troubleshooting

A common approach to improve the accumulation of NIR probes at the target site is to conjugate the fluorophores to a ligand (small molecules, peptides, proteins or antibodies) that binds to a specific molecular target. In these cases, the probes bind the targets and are retained at the target site, while non-bound probes are cleared from the circulation.(Zhao, et al., 2008) This approach has proven to be useful for tumor imaging because tumor cells often overexpress certain surface receptors.(Mankoff, et al., 2008)

It is often necessary to image treated cells at multiple laser powers and voltages to determine the optimum settings for imaging each probe. It is best to capture preliminary images in a fast scan mode to minimize photobleaching during the optimization process. At high concentrations fluorescent dyes can quench, resulting in a decrease or absence of fluorescent signal. Thus, it may appear that a dye has not internalized when it actually has internalized very well. Quenching can be detected by testing fluorescent probes at a range of concentrations. Confocal microscope software systems allow users to adjust the window of emission wavelengths that are collected. This is useful when imaging with multiple fluorophores that have emission spectra that are close to each other, reducing spectral overlap.

For in vivo studies, a simple method for selecting ROIs for ex vivo tissues is to first find the tissues on the brightfield image using thresholding and the “magic wand” tool, then transferring the ROI fields to the corresponding fluorescence image. This method reduces

human error in selecting the ROIs from the fluorescence image alone, which may not adequately map out the full tissue area.

Histograms of the fitted lifetimes can aid separation of fluorophore lifetimes for lifetime-gated representation of the data as separate images for localization of different lifetimes, either due to physiological differences within the mouse, or due to injection of multiple imaging agents. Small changes in tissue physiology may affect the fluorescence lifetime of single fluorophores.

Anticipated Results

For in vitro imaging, intracellular fluorescence of internalized probes can range from 2 fold to 20 fold higher than that of untreated cells. Fluorescence may appear diffuse, suggesting the probe is dispersed throughout the cytosol, or punctuate, indicating the probe is sequestered in organelles such as lysosomes or endosomes. Some probes bind to the surface of cells but are not internalized, creating a fluorescent outline of the cell.

The average ratio of tumor fluorescence to that of muscle is generally reported for each group to assess target selectivity assuming expression of the target is relatively low in muscle tissue. In general, fluorescence intensity should be greater than 3-fold higher in target tissue relative to non-target to demonstrate selectivity, particularly in tumor xenograft models where nonspecific accumulation can artificially increase contrast. Calculated fluorescence lifetime values should be compared with in vitro measurements as a quality check.

Statistical Analysis—Statistical analysis using the two-sided Student's t test is generally performed to compare mean fluorescence intensity and lifetime values for each set with $\alpha = 0.05$. It is typical for measurements to vary by anatomic region and physiologic conditions within the body, depending on the sensitivity of the NIR dye.

Time Considerations

In vitro imaging can be performed on cells treated for a few minutes to cells treated for several days. Cells can generally survive outside of the incubator for an hour or so before they begin to lift off of the slide. Thus, once imaging is begun it should be completed within an hour. For longitudinal studies during which the cells are imaged over several hours, microscopes can be equipped with a heated stage and CO_2 chamber.

The time to complete an in vivo imaging study is highly dependent on the pharmacokinetics of the molecular imaging agent. For example, imaging with antibody-based molecular probes requires 3–5 days for optimal contrast due to the long circulation time and therefore background signal. Small MW molecular probes based on peptide sequences or peptidomimetics clear faster and can provide selective contrast in 1–24 hr.

Acknowledgments

The authors thank the National Institute of Biological Imaging and Bioengineering (NIBIB R01 EB008111, R01 EB008458, R01 EB007276), the National Cancer Institute (NCI R33 CA123537, U54 CA136398), and the National Heart, Lung and Blood Institute Program of Excellence in Nanotechnology (HHSN268201000046C) of the US National Institutes of Health for financial support.

Literature Cited

Achilefu S. The Insatiable Quest for Near-Infrared Fluorescent Probes for Molecular Imaging. Angewandte Chemie-International Edition. 2010; 49:9816–9818.

Achilefu S, Bloch S, Markiewicz MA, Zhong TX, Ye YP, Dorshow RB, Chance B, Liang KX. Synergistic effects of light-emitting probes and peptides for targeting and monitoring integrin expression. Proceedings of the National Academy of Sciences of the United States of America. 2005; 102:7976–7981. [PubMed: 15911748]

Achilefu S, Dorshow RB, Bugaj JE, Rajagopalan R. Novel receptor-targeted fluorescent contrast agents for in vivo tumor imaging. Invest Radiol. 2000; 35:479–485. [PubMed: 10946975]

Akers WJ, Kim C, Berezin M, Guo K, Fuhrhop R, Lanza GM, Fischer GM, Daltrozzo E, Zumbusch A, Cai X, et al. Noninvasive photoacoustic and fluorescence sentinel lymph node identification using dye-loaded perfluorocarbon nanoparticles. ACS Nano. 2011; 5:173–182. [PubMed: 21171567]

Akers WJ, Zhang Z, Berezin M, Ye Y, Agee A, Guo K, Fuhrhop RW, Wickline SA, Lanza GM, Achilefu S. Targeting of alpha(nu)beta(3)-integrins expressed on tumor tissue and neovasculature using fluorescent small molecules and nanoparticles. Nanomedicine (Lond). 2010; 5:715–726. [PubMed: 20662643]

Alian W, Andersson-Engels S, Svanberg K, Svanberg S. Laser-induced fluorescence studies of meso-tetra(hydroxyphenyl)chlorin in malignant and normal tissues in rats. Br J Cancer. 1994; 70:880–885. [PubMed: 7947093]

Altınoğlu EI, Russin TJ, Kaiser JM, Barth BM, Eklund PC, Kester M, Adair JH. Near-Infrared Emitting Fluorophore-Doped Calcium Phosphate Nanoparticles for In Vivo Imaging of Human Breast Cancer. ACS Nano. 2008; 2:2075–2084. [PubMed: 19206454]

Andersson-Engels S, Ankerst J, Johansson J, Svanberg K, Svanberg S. Laser-induced fluorescence in malignant and normal tissue of rats injected with benzoporphyrin derivative. Photochem Photobiol. 1993; 57:978–983. [PubMed: 8367537]

Arunkumar E, Forbes CC, Noll BC, Smith BD. Squaraine-derived rotaxanes: sterically protected fluorescent near-IR dyes. J Am Chem Soc. 2005; 127:3288–3289. [PubMed: 15755140]

Arunkumar E, Fu N, Smith BD. Squaraine-derived rotaxanes: highly stable, fluorescent near-IR dyes. Chemistry. 2006; 12:4684–4690. [PubMed: 16575935]

Bakshi MS, Sharma P, Banipal TS, Kaur G, KanjiroTorigoe, Petersen NO, Possmayer F. Lamellar phase supported synthesis of colloidal gold nanoparticles, nanoclusters, and nanowires. J Nanosci Nanotechnol. 2007; 7:916–924. [PubMed: 17450854]

Ballou B, Ernst LA, Waggoner AS. Fluorescence imaging of tumors in vivo. Current Medicinal Chemistry. 2005; 12:795–805. [PubMed: 15853712]

Berezin MY, Akers WJ, Guo K, Fischer GM, Daltrozzo E, Zumbusch A, Achilefu S. Long Fluorescence Lifetime Molecular Probes Based on Near Infrared Pyrrolopyrrole Cyanine Fluorophores for In Vivo Imaging. Biophysical Journal. 2009; 97:L22–L24. [PubMed: 19883579]

Berezin MY, Akers WJ, Guo K, Fischer GM, Daltrozzo E, Zumbusch A, Achilefu S. Long fluorescence lifetime molecular probes based on near infrared pyrrolopyrrole cyanine fluorophores for in vivo imaging. Biophys J. 2009; 97:L22–L24. [PubMed: 19883579]

Bremer C, Tung CH, Weissleder R. In vivo molecular target assessment of matrix metalloproteinase inhibition. Nature Medicine. 2001; 7:743–748.

Bugaj JE, Achilefu S, Dorshow RB, Rajagopalan R. Novel fluorescent contrast agents for optical imaging of in vivo tumors based on a receptor-targeted dye-peptide conjugate platform. J Biomed Opt. 2001; 6:122–133. [PubMed: 11375721]

Cai W, Shin DW, Chen K, Gheysens O, Cao Q, Wang SX, Gambhir SS, Chen X. Peptide-labeled near-infrared quantum dots for imaging tumor vasculature in living subjects. Nano Lett. 2006; 6:669–676. [PubMed: 16608262]

Cheng Z, Wu Y, Xiong ZM, Gambhir SS, Chen XY. Near-infrared fluorescent RGD peptides for optical imaging of integrin alpha(v)beta 3 expression in living mice. Bioconjugate Chemistry. 2005; 16:1433–1441. [PubMed: 16287239]

Chopra A. Humanized anti-type 1 insulin-like growth factor receptor monoclonal antibody conjugated to Alexa 680. 2004

Conway CL, Walker I, Bell A, Roberts DJ, Brown SB, Vernon DI. In vivo and in vitro characterisation of a protoporphyrin IX-cyclic RGD peptide conjugate for use in photodynamic therapy. Photochem Photobiol Sci. 2008; 7:290–298. [PubMed: 18389145]

Cooper ME, Gregory S, Adie E, Kalinka S. pH-sensitive cyanine dyes for biological applications. Journal of Fluorescence. 2002; 12:425–429.

Costantino L, Gandolfi F, Tosi G, Rivasi F, Vandelli MA, Forni F. Peptide-derivatized biodegradable nanoparticles able to cross the blood-brain barrier. Journal of Controlled Release. 2005; 108:84–96. [PubMed: 16154222]

Cubeddu R, Pifferi A, Taroni P, Torricelli A, Valentini G, Comelli D, D'Andrea C, Angelini V, Canti G. Fluorescence imaging during photodynamic therapy of experimental tumors in mice sensitized with disulfonated aluminum phthalocyanine. Photochem Photobiol. 2000; 72:690–695. [PubMed: 11107856]

Diagaradjane P, Orenstein-Cardona JM, Colon-Casasnovas NE, Deorukhkar A, Shentu S, Kuno N, Schwartz DL, Gelovani JG, Krishnan S. Imaging epidermal growth factor receptor expression in vivo: pharmacokinetic and biodistribution characterization of a bioconjugated quantum dot nanoprobe. Clin Cancer Res. 2008; 14:731–741. [PubMed: 18245533]

Dijkgraaf I, Beer AJ, Wester HJ. Application of RGD-containing peptides as imaging probes for alphavbeta3 expression. Front Biosci. 2009; 14:887–899. [PubMed: 19273106]

Dorozhkin SV, Epple M. Biological and medical significance of calcium phosphates. Angew Chem Int Ed Engl. 2002; 41:3130–3146. [PubMed: 12207375]

Dougherty TJ, Gomer CJ, Weishaupt KR. Energetics and efficiency of photoinactivation of murine tumor cells containing hematoporphyrin. Cancer Res. 1976; 36:2330–2333. [PubMed: 1277138]

Escobedo JO, Rusin O, Lim S, Strongin RM. NIR dyes for bioimaging applications. Current Opinion in Chemical Biology. 2010; 14:64–70. [PubMed: 19926332]

Fischer GM, Isomaki-Krondahl M, Gottker-Schnetmann I, Daltrozzo E, Zumbusch A. Pyrrolopyrrole Cyanine Dyes: A New Class of Near-Infrared Dyes and Fluorophores. Chemistry-a European Journal. 2009; 15:4857–4864.

Fischer GM, Jungst C, Isomaki-Krondahl M, Gauss D, Moller HM, Daltrozzo E, Zumbusch A. Asymmetric PPCys: strongly fluorescing NIR labels. Chem Commun (Camb). 2010; 46:5289–5291. [PubMed: 20539898]

Funovics M, Weissleder R, Tung CH. Protease sensors for bioimaging. Anal Bioanal Chem. 2003; 377:956–963. [PubMed: 12955390]

Gao J, Chen K, Xie R, Xie J, Lee S, Cheng Z, Peng X, Chen X. Ultrasmall near-infrared non-cadmium quantum dots for in vivo tumor imaging. Small. 2010; 6:256–261. [PubMed: 19911392]

Ghoroghchian PP, Frail PR, Susumu K, Blessington D, Brannan AK, Bates FS, Chance B, Hammer DA, Therien MJ. Near-infrared-emissive polymersomes: self-assembled soft matter for in vivo optical imaging. Proc Natl Acad Sci U S A. 2005; 102:2922–2927. [PubMed: 15708979]

Gompels LL, Madden L, Lim NH, Inglis JJ, McConnell E, Vincent TL, Haskard DO, Paleolog EM. In vivo fluorescence imaging of E-selectin: quantitative detection of endothelial activation in a mouse model of arthritis. Arthritis Rheum. 2011; 63:107–117. [PubMed: 20954188]

Gurfinkel M, Thompson AB, Ralston W, Troy TL, Moore AL, Moore TA, Gust JD, Tatman D, Reynolds JS, Muggenburg B, et al. Pharmacokinetics of ICG and HPPH-car for the detection of normal and tumor tissue using fluorescence, near-infrared reflectance imaging: A case study. Photochemistry and Photobiology. 2000; 72:94–102. [PubMed: 10911733]

Hama Y, Koyama Y, Urano Y, Choyke PL, Kobayashi H. Simultaneous two-color spectral fluorescence lymphangiography with near infrared quantum dots to map two lymphatic flows from the breast and the upper extremity. Breast Cancer Res Treat. 2007; 103:23–28. [PubMed: 17028977]

Hardman R. A toxicologic review of quantum dots: toxicity depends on physicochemical and environmental factors. Environ Health Perspect. 2006; 114:165–172. [PubMed: 16451849]

He X, Gao J, Gambhir SS, Cheng Z. Near-infrared fluorescent nanoprobes for cancer molecular imaging: status and challenges. Trends Mol Med. 2010; 16:574–583. [PubMed: 20870460]

He X, Wang K, Cheng Z. In vivo near-infrared fluorescence imaging of cancer with nanoparticle-based probes. Wiley Interdiscip Rev Nanomed Nanobiotechnol. 2010; 2:349–366. [PubMed: 20564463]

He XX, Gao JH, Gambhir SS, Cheng Z. Near-infrared fluorescent nanoprobes for cancer molecular imaging: status and challenges. Trends in Molecular Medicine. 2010; 16:574–583. [PubMed: 20870460]

Hewett J, Nadeau V, Ferguson J, Moseley H, Ibbotson S, Allen JW, Sibbett W, Padgett M. The application of a compact multispectral imaging system with integrated excitation source to in vivo monitoring of fluorescence during topical photodynamic therapy of superficial skin cancers. Photochem Photobiol. 2001; 73:278–282. [PubMed: 11281024]

Hilderbrand SA, Kelly KA, Niedre M, Weissleder R. Near infrared fluorescence-based bacteriophage particles for ratiometric pH imaging. Bioconjug Chem. 2008; 19:1635–1639. [PubMed: 18666791]

Hilderbrand SA, Weissleder R. Near-infrared fluorescence: application to in vivo molecular imaging. Current Opinion in Chemical Biology. 2010; 14:71–79. [PubMed: 19879798]

Hilderbrand SA, Weissleder R. NearNear-infrared fluorescence: application to in vivo molecular imaging. Current Opinion in Chemical Chemical Biology. 2010; 1414:7171–7179.

Hong H, Zhang Y, Cai W. In vivo imaging of RNA interference. J Nucl Med. 2010; 51:169–172. [PubMed: 20080892]

Huang CC, Chen CT, Shiang YC, Lin ZH, Chang HT. Synthesis of fluorescent carbohydrate-protected Au nanodots for detection of Concanavalin A and Escherichia coli. Anal Chem. 2009; 81:875–882. [PubMed: 19119843]

Jin T, Fujii F, Komai Y, Seki J, Seiyama A, Yoshioka Y. Preparation and characterization of highly fluorescent, glutathione-coated near infrared quantum dots for in vivo fluorescence imaging. Int J Mol Sci. 2008; 9:2044–2061. [PubMed: 19325735]

Johnson JR, Fu N, Arunkumar E, Leevy WM, Gammon ST, Piwnica-Worms D, Smith BD. Squaraine rotaxanes: superior substitutes for Cy-5 in molecular probes for near-infrared fluorescence cell imaging. Angew Chem Int Ed Engl. 2007; 46:5528–5531. [PubMed: 17585399]

Ke S, Wen X, Gurfinkel M, Charnsangavej C, Wallace S, Sevick-Muraca EM, Li C. Near-infrared optical imaging of epidermal growth factor receptor in breast cancer xenografts. Cancer Res. 2003; 63:7870–7875. [PubMed: 14633715]

Kim S, Lim YT, Soltesz EG, De Grand AM, Lee J, Nakayama A, Parker JA, Mihaljevic T, Laurence RG, Dor DM, et al. Near-infrared fluorescent type II quantum dots for sentinel lymph node mapping. Nat Biotechnol. 2004; 22:93–97. [PubMed: 14661026]

Kobayashi H, Choyke PL. Target-Cancer-Cell-Specific Activatable Fluorescence Imaging Probes: Rational Design and in Vivo Applications. Accounts of Chemical Research. 2011; 44:83–90. [PubMed: 21062101]

Kobayashi H, Koyama Y, Barrett T, Hama Y, Regino CAS, Shin IS, Jang BS, Le N, Paik CH, Choyke PL, et al. Multimodal nanoprobes for radionuclide and five-color near-infrared optical lymphatic imaging. Acs Nano. 2007; 1:258–264. [PubMed: 19079788]

Komatsu T, Kikuchi K, Takakusa H, Hanaoka K, Ueno T, Kamiya M, Urano Y, Nagano T. Design and synthesis of an enzyme activity-based labeling molecule with fluorescence spectral change. J Am Chem Soc. 2006; 128:15946–15947. [PubMed: 17165702]

Kosaka N, Mitsunaga M, Longmire MR, Choyke PL, Kobayashi H. Near infrared fluorescence-guided real-time endoscopic detection of peritoneal ovarian cancer nodules using intravenously injected indocyanine green. Int J Cancer. 2011

Kundu K, Knight SF, Willett N, Lee S, Taylor WR, Murthy N. Hydrocyanines: a class of fluorescent sensors that can image reactive oxygen species in cell culture, tissue, and in vivo. Angew Chem Int Ed Engl. 2009; 48:299–303. [PubMed: 19065548]

Lakowicz JR. Principles of frequency-domain fluorescence spectroscopy and applications to cell membranes. Subcell Biochem. 1988; 13:89–126. [PubMed: 2577864]

Lee C-H, Cheng S-H, Wang Y-J, Chen Y-C, Chen N-T, Souris J, Chen C-T, Mou C-Y, Yang C-S, Lo L-W. Near-Infrared Mesoporous Silica Nanoparticles for Optical Imaging: Characterization and In Vivo Biodistribution. Advanced Functional Materials. 2009; 19:215–222.

Lee H, Akers W, Bhushan K, Bloch S, Sudlow G, Tang R, Achilefu S. Near-Infrared pH-Activatable Fluorescent Probes for Imaging Primary and Metastatic Breast Tumors. Bioconjug Chem. 2011; 22:777–784. [PubMed: 21388195]

Lee H, Akers WJ, Cheney PP, Edwards WB, Liang K, Culver JP, Achilefu S. Complementary optical and nuclear imaging of caspase-3 activity using combined activatable and radio-labeled multimodality molecular probe. J Biomed Opt. 2009; 14 040507.

Leung K. Anti-vascular cell adhesion molecule-1 monoclonal antibody M/K-2.7 microbubbles. 2004

Leung K. IRDye 800-Labeled anti-epidermal growth factor receptor Affibody. 2004

Li L, Qian H, Ren J. Rapid synthesis of highly luminescent CdTe nanocrystals in the aqueous phase by microwave irradiation with controllable temperature. Chem Commun (Camb). 2005:528–530. [PubMed: 15654392]

Licha K. Contrast agents for optical imaging. Contrast Agents Ii. 2002; 222:1–29.

Licha K, Riefke B, Ntziachristos V, Becker A, Chance B, Semmler W. Hydrophilic cyanine dyes as contrast agents for near-infrared tumor imaging: Synthesis, photophysical properties and spectroscopic in vivo characterization. Photochemistry and Photobiology. 2000; 72:392–398. [PubMed: 10989611]

Linder KE, Metcalfe E, Nanjappan P, Arunachalam T, Ramos K, Skedzielewski TM, Tweedle MF, Nunn AD, Swenson RE. Synthesis, In Vitro Evaluation and In Vivo Metabolism of Fluor/Quencher Compounds Containing IRDye 800CW and Black Hole Quencher-3 (BHQ-3). Bioconjug Chem. 2011

Liu Z, Tabakman S, Welsher K, Dai H. Carbon Nanotubes in Biology and Medicine: In vitro and in vivo Detection, Imaging and Drug Delivery. Nano Res. 2009; 2:85–120. [PubMed: 20174481]

Ma N, Marshall AF, Rao J. Near-infrared light emitting luciferase via biomineralization. J Am Chem Soc. 2010; 132:6884–6885. [PubMed: 20441172]

Mankoff DA, Link JM, Linden HM, Sundararajan L, Krohn KA. Tumor receptor imaging. J Nucl Med. 2008; 49(Suppl 2):149S–163S. [PubMed: 18523071]

Matsumura Y, Maeda H. A new concept for macromolecular therapeutics in cancer chemotherapy: mechanism of tumoritropic accumulation of proteins and the antitumor agent smancs. Cancer Res. 1986; 46:6387–6392. [PubMed: 2946403]

Meek ST, Nesterov EE, Swager TM. Near-infrared fluorophores containing benzo[c]heterocycle subunits. Org Lett. 2008; 10:2991–2993. [PubMed: 18563902]

Morgan NY, English S, Chen W, Chernomordik V, Russo A, Smith PD, Gandjbakhche A. Real time in vivo non-invasive optical imaging using near-infrared fluorescent quantum dots. Acad Radiol. 2005; 12:313–323. [PubMed: 15766692]

Murari K, Zhang YY, Li SP, Chen YP, Li MJ, Li XD. Compensation-free, all-fiber-optic, two-photon endomicroscopy at 1.55 mu m. Optics Letters. 2011; 36:1299–1301. [PubMed: 21479064]

Nesterov EE, Skoch J, Hyman BT, Klunk WE, Bacskai BJ, Swager TM. In vivo optical imaging of amyloid aggregates in brain: design of fluorescent markers. Angew Chem Int Ed Engl. 2005; 44:5452–5456. [PubMed: 16059955]

O'Connell MJ, Bachilo SM, Huffman CB, Moore VC, Strano MS, Haroz EH, Rialon KL, Boul PJ, Noon WH, Kittrell C, et al. Band gap fluorescence from individual single-walled carbon nanotubes. Science. 2002; 297:593–596. [PubMed: 12142535]

Ochsner M. Photophysical and photobiological processes in the photodynamic therapy of tumours. J Photochem Photobiol B. 1997; 39:1–18. [PubMed: 9210318]

Ogawa M, Kosaka N, Choyke PL, Kobayashi H. In vivo molecular imaging of cancer with a quenching near-infrared fluorescent probe using conjugates of monoclonal antibodies and indocyanine green. Cancer Res. 2009; 69:1268–1272. [PubMed: 19176373]

Owens SL. Indocyanine green angiography. British Journal of Ophthalmology. 1996; 80:263–266. [PubMed: 8703866]

Peng Q, Warloe T, Berg K, Moan J, Kongshaug M, Giercksky KE, Nesland JM. 5-Aminolevulinic acid-based photodynamic therapy. Clinical research and future challenges. Cancer. 1997; 79:2282–2308. [PubMed: 9191516]

Peng X, Chen H, Draney DR, Volcheck W, Schutz-Geschwender A, Olive DM. A nonfluorescent, broad-range quencher dye for Forster resonance energy transfer assays. Anal Biochem. 2009; 388:220–228. [PubMed: 19248753]

Peng ZA, Peng X. Formation of high-quality CdTe, CdSe, and CdS nanocrystals using CdO as precursor. J Am Chem Soc. 2001; 123:183–184. [PubMed: 11273619]

Povrozin YA, Markova LI, Tatarets AL, Sidorov VI, Terpetschnig EA, Patsenker LD. Near-infrared, dual-ratiometric fluorescent label for measurement of pH. Anal Biochem. 2009; 390:136–140. [PubMed: 19351524]

Qian H, Qiu X, Li L, Ren J. Microwave-assisted aqueous synthesis: a rapid approach to prepare highly luminescent ZnSe(S) alloyed quantum dots. J Phys Chem B. 2006; 110:9034–9040. [PubMed: 16671712]

Rao JH, Dragulescu-Andrasi A, Yao HQ, Yao HQ. Fluorescence imaging in vivo: recent advances. Current Opinion in Biotechnology. 2007; 18:17–25. [PubMed: 17234399]

Sameiro M, Goncalves T. Fluorescent Labeling of Biomolecules with Organic Probes. Chemical Reviews. 2009; 109:190–212. [PubMed: 19105748]

Sampath L, Kwon S, Ke S, Wang W, Schiff R, Mawad ME, Sevick-Muraca EM. Dual-labeled trastuzumab-based imaging agent for the detection of human epidermal growth factor receptor 2 overexpression in breast cancer. J Nucl Med. 2007; 48:1501–1510. [PubMed: 17785729]

Santra S, Dutta D, Walter GA, Moudgil BM. Fluorescent nanoparticle probes for cancer imaging. Technol Cancer Res Treat. 2005; 4:593–602. [PubMed: 16292879]

Santra S, Wang K, Tapec R, Tan W. Development of novel dye-doped silica nanoparticles for biomarker application. J Biomed Opt. 2001; 6:160–166. [PubMed: 11375725]

Schenke-Layland K, Riemann I, Stock UA, Konig K. Imaging of cardiovascular structures using near-infrared femtosecond multiphoton laser scanning microscopy. J Biomed Opt. 2005; 10 024017.

Schenke-Layland K, Vasilevski O, Opitz F, Konig K, Riemann I, Halbhuber KJ, Wahlers T, Stock UA. Impact of decellularization of xenogeneic tissue on extracellular matrix integrity for tissue engineering of heart valves. J Struct Biol. 2003; 143:201–208. [PubMed: 14572475]

Sevick-Muraca EM, Houston JP, Gurfinkel M. Fluorescence-enhanced, near infrared diagnostic imaging with contrast agents. Curr. Opin. Chem. Biol. 2002; 6:642–650. [PubMed: 12413549]

Shao X, Zheng W, Huang Z. Polarized near-infrared autofluorescence imaging combined with near-infrared diffuse reflectance imaging for improving colonic cancer detection. Opt Express. 2010; 18:24293–24300. [PubMed: 21164775]

Smith AM, Duan H, Mohs AM, Nie S. Bioconjugated quantum dots for in vivo molecular and cellular imaging. Adv Drug Deliv Rev. 2008; 60:1226–1240. [PubMed: 18495291]

Smith BR, Cheng Z, De A, Koh AL, Sinclair R, Gambhir SS. Real-time intravital imaging of RGD-quantum dot binding to luminal endothelium in mouse tumor neovasculature. Nano Lett. 2008; 8:2599–2606. [PubMed: 18386933]

So MK, Loening AM, Gambhir SS, Rao J. Creating self-illuminating quantum dot conjugates. Nat Protoc. 2006; 1:1160–1164. [PubMed: 17406398]

So MK, Xu C, Loening AM, Gambhir SS, Rao J. Self-illuminating quantum dot conjugates for in vivo imaging. Nat Biotechnol. 2006; 24:339–343. [PubMed: 16501578]

Tang B, Yu F, Li P, Tong L, Duan X, Xie T, Wang X. A near-infrared neutral pH fluorescent probe for monitoring minor pH changes: imaging in living HepG2 and HL-7702 cells. J Am Chem Soc. 2009; 131:3016–3023. [PubMed: 19199620]

Tavares AJ, Chong L, Petryayeva E, Algar WR, Krull UJ. Quantum dots as contrast agents for in vivo tumor imaging: progress and issues. Anal Bioanal Chem. 2011; 399:2331–2342. [PubMed: 20658228]

Tosi G, Bondioli L, Ruozi B, Badiali L, Severini GM, Biffi S, De Vita A, Bortot B, Dolcetta D, Forni F, et al. NIR-labeled nanoparticles engineered for brain targeting: in vivo optical imaging application and fluorescent microscopy evidences. J Neural Transm. 2011; 118:145–153. [PubMed: 20931242]

Tosi G, Bondioli L, Ruozi B, Badiali L, Severini GM, Biffi S, De Vita A, Bortot B, Dolcetta D, Forni F, et al. NIR-labeled nanoparticles engineered for brain targeting: in vivo optical imaging application and fluorescent microscopy evidences. Journal of Neural Transmission. 2011; 118:145–153. [PubMed: 20931242]

Umezawa K, Matsui A, Nakamura Y, Citterio D, Suzuki K. Bright, color-tunable fluorescent dyes in the Vis/NIR region: establishment of new "tailor-made" multicolor fluorophores based on borondipyrromethene. Chemistry. 2009; 15:1096–1106. [PubMed: 19117043]

Umezawa K, Nakamura Y, Makino H, Citterio D, Suzuki K. Bright, color-tunable fluorescent dyes in the visible-near-infrared region. J Am Chem Soc. 2008; 130:1550–1551. [PubMed: 18193873]

Urano Y, Asanuma D, Hama Y, Koyama Y, Barrett T, Kamiya M, Nagano T, Watanabe T, Hasegawa A, Choyke PL, et al. Selective molecular imaging of viable cancer cells with pH-activatable fluorescence probes. Nat Med. 2009; 15:104–109. [PubMed: 19029979]

Wang K, Wang K, Li W, Huang T, Li R, Wang D, Shen B, Chen X. Characterizing breast cancer xenograft epidermal growth factor receptor expression by using near-infrared optical imaging. Acta Radiol. 2009; 50:1095–1103. [PubMed: 19922304]

Xiao Y, Gao X, Taratula O, Treado S, Urbas A, Holbrook RD, Cavicchi RE, Avedisian CT, Mitra S, Savla R, et al. Anti-HER2 IgY antibody-functionalized single-walled carbon nanotubes for detection and selective destruction of breast cancer cells. BMC Cancer. 2009; 9:351. [PubMed: 19799784]

Xie J, Zheng Y, Ying JY. Protein-directed synthesis of highly fluorescent gold nanoclusters. J Am Chem Soc. 2009; 131:888–889. [PubMed: 19123810]

Xing Y, Xia Z, Rao J. Semiconductor quantum dots for biosensing and in vivo imaging. IEEE Trans Nanobioscience. 2009; 8:4–12. [PubMed: 19304495]

Yang Y, Lowry M, Xu X, Escobedo JO, Sibrian-Vazquez M, Wong L, Schowalter CM, Jensen TJ, Fronczek FR, Warner IM, et al. Seminaphthofluorones are a family of water-soluble, low molecular weight, NIR-emitting fluorophores. Proc Natl Acad Sci U S A. 2008; 105:8829–8834. [PubMed: 18579790]

Yazdanfar S, Joo C, Zhan C, Berezin MY, Akers WJ, Achilefu S. Multiphoton microscopy with near infrared contrast agents. Journal of Biomedical Optics. 2010; 15

Ye Y, Bloch S, Xu B, Achilefu S. Novel near-infrared fluorescent integrin-targeted DFO analogue. Bioconjug Chem. 2008; 19:225–234. [PubMed: 18038965]

Ye YP, Bloch S, Xu BG, Achilefu S. Design, synthesis, and evaluation of near infrared fluorescent multimeric RGD peptides for targeting tumors. Journal of Medicinal Chemistry. 2006; 49:2268–2275. [PubMed: 16570923]

Ying LQ, Branchaud BP. Facile synthesis of symmetric, monofunctional cyanine dyes for imaging applications. Bioconjug Chem. 2011; 22:865–869. [PubMed: 21517120]

Zhang Z, Achilefu S. Design, synthesis and evaluation of near-infrared fluorescent pH indicators in a physiologically relevant range. Chem Commun (Camb). 2005:5887–5889. [PubMed: 16317464]

Zhang Z, Fan J, Cheney PP, Berezin MY, Edwards WB, Akers WJ, Shen D, Liang K, Culver JP, Achilefu S. Activatable Molecular Systems Using Homologous Near-Infrared Fluorescent Probes for Monitoring Enzyme Activities in Vitro, in Cellulo, and in Vivo. Molecular Pharmaceutics. 2009; 6:416–427. [PubMed: 19718795]

Zhao H, Cui K, Muschenborn A, Wong ST. Progress of engineered antibody-targeted molecular imaging for solid tumors (Review). Mol Med Report. 2008; 1:131–134. [PubMed: 21479389]

Zheng J, Nicovich PR, Dickson RM. Highly fluorescent noble-metal quantum dots. Annu Rev Phys Chem. 2007; 58:409–431. [PubMed: 17105412]

Zheng J, Petty JT, Dickson RM. High quantum yield blue emission from water-soluble Au8 nanodots. J Am Chem Soc. 2003; 125:7780–7781. [PubMed: 12822978]

Zheng Q, Xu G, Prasad PN. Conformationally restricted dipyrromethene boron difluoride (BODIPY) dyes: highly fluorescent, multicolored probes for cellular imaging. Chemistry. 2008; 14:5812–5819. [PubMed: 18494008]

Zou P, Xu S, Povoski SP, Wang A, Johnson MA, Martin EW Jr. Subramaniam V, Xu R, Sun D. Near-infrared fluorescence labeled anti-TAG-72 monoclonal antibodies for tumor imaging in colorectal cancer xenograft mice. Mol Pharm. 2009; 6:428–440. [PubMed: 19718796]

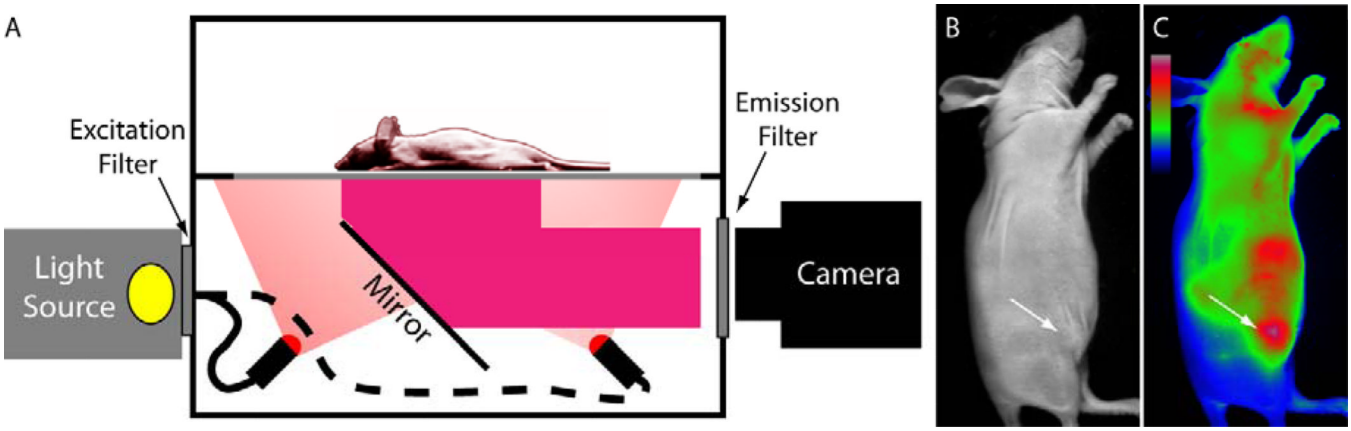

Figure 1.

(A) Simplified schematic of a preclinical planar fluorescence reflectance imaging system with light source, imaging chamber and digital camera for detection. The wavelengths of excitation and emission collection can be selected with optical bandpass filters. (B) Brightfield image of mouse with subcutaneous tumor in left flank. (C) Fluorescence image of same mouse showing signal from NIR fluorescent molecular probe IntegriSense 680 (center wavelenth of filters: excitation 630 nm, emission 700 nm)

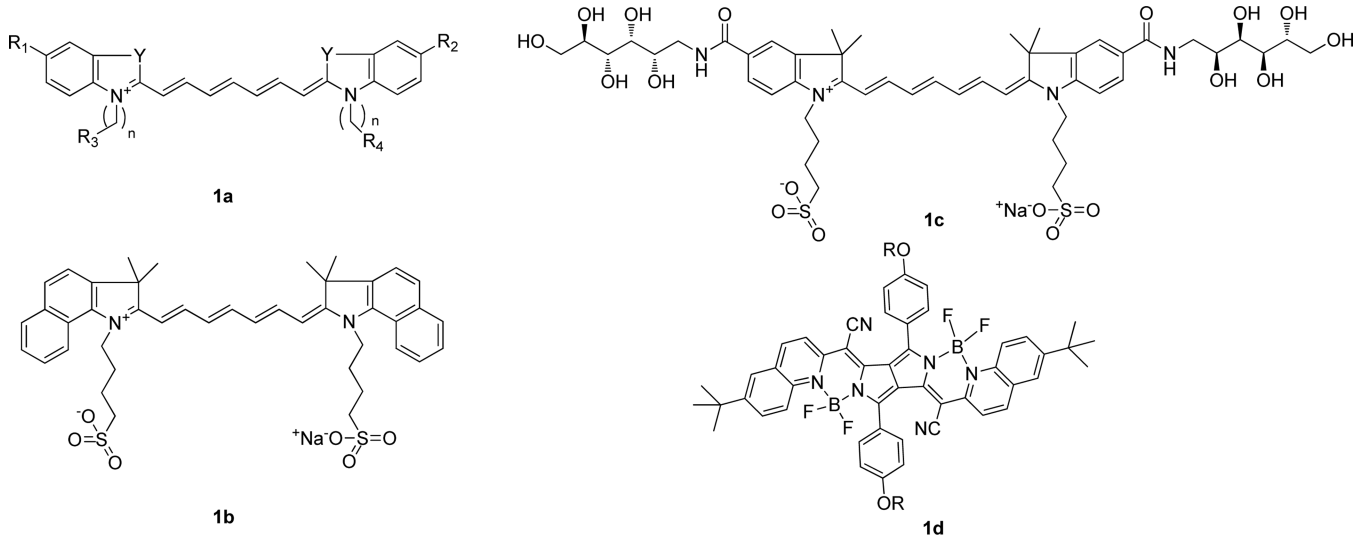

Figure 2.
Structures of a) cyanine, b) ICG, c) SIDAG, d) PPCy.

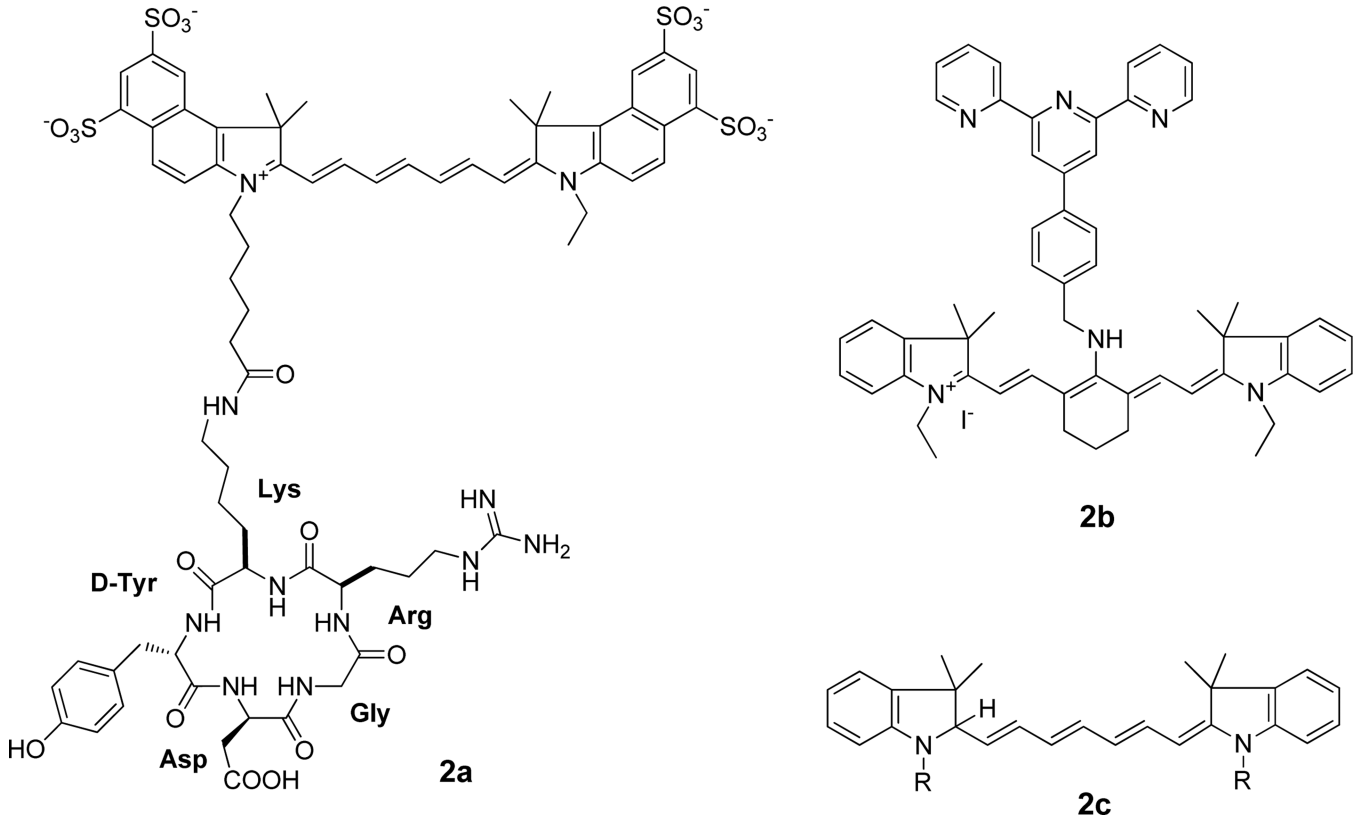

Figure 3.
New NIR cyanines. a) cyanine with RGD peptide, b) pH-sensitive cyanines, c) ROS cyanine.

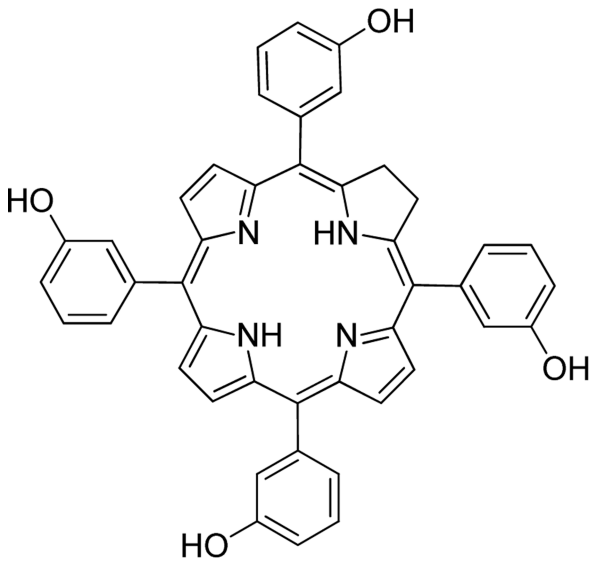

3a

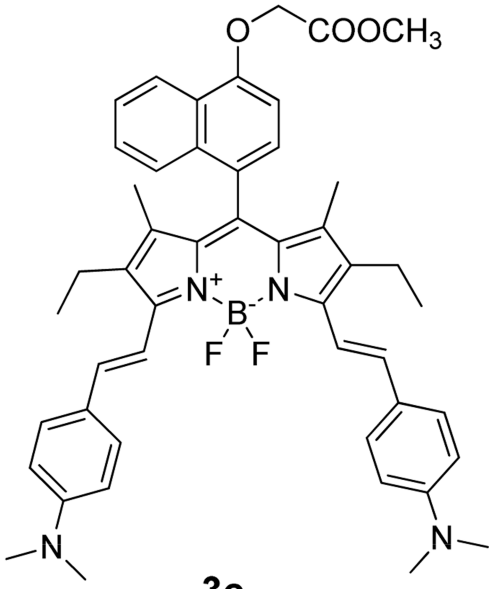

3c

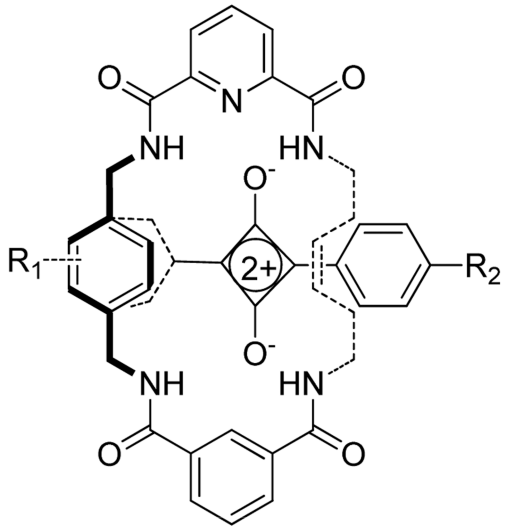

3b

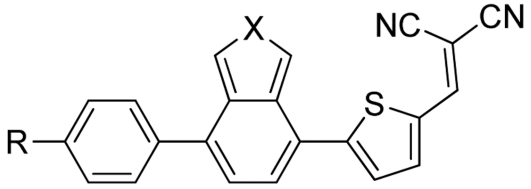

X = S, O

R = H, MeO, OH or $N(Me)_2$

3d

Figure 4.
Structures of representative miscellaneous NIR dyes. a) *m*-THPC, b) squaraine, c) BODIPY, d) push-pull-type NIR dye

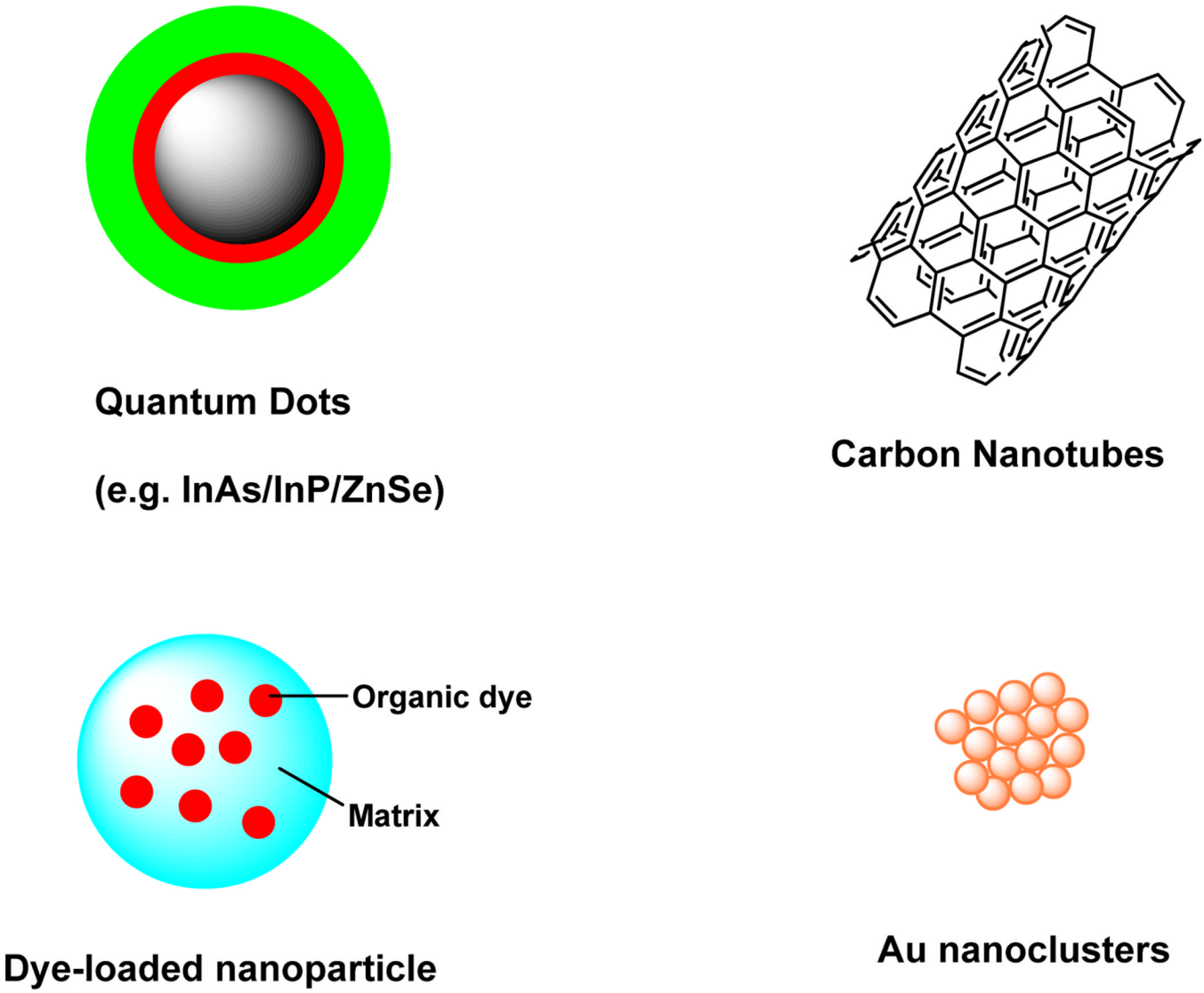

Figure 5.
Representative nanoparticle-based NIR probes for biological imaging.

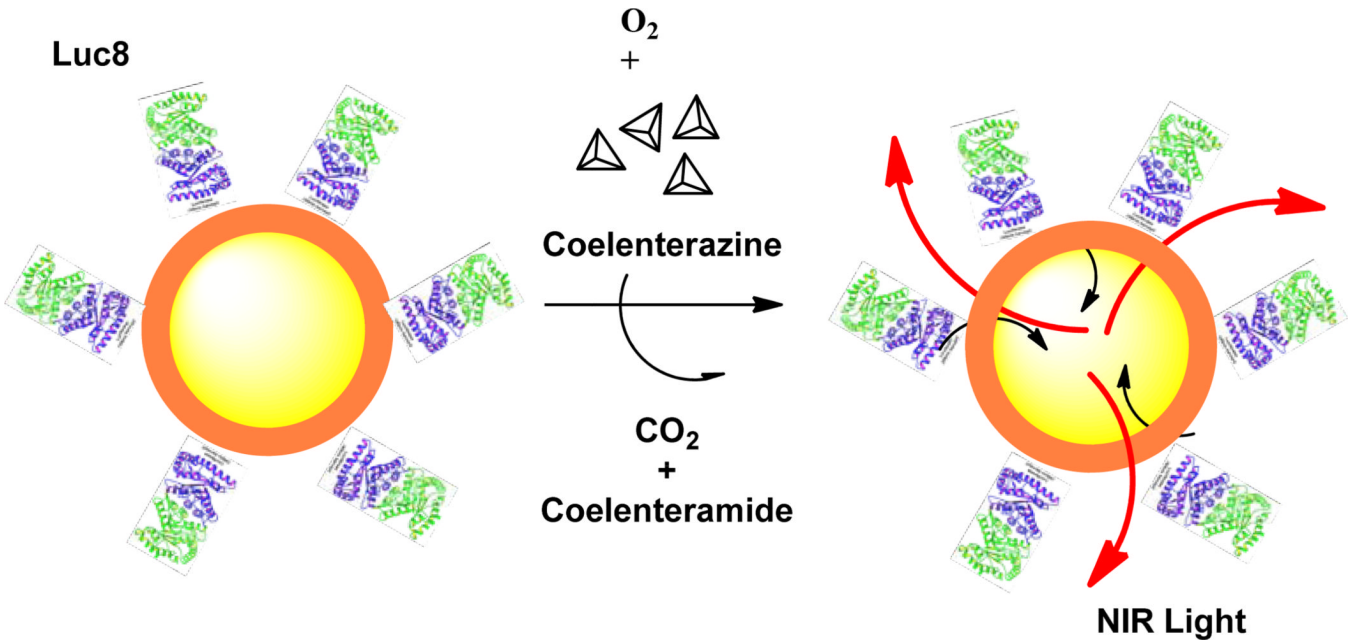

Figure 6.
Schematic illustration of self-illuminating NIR QDs.

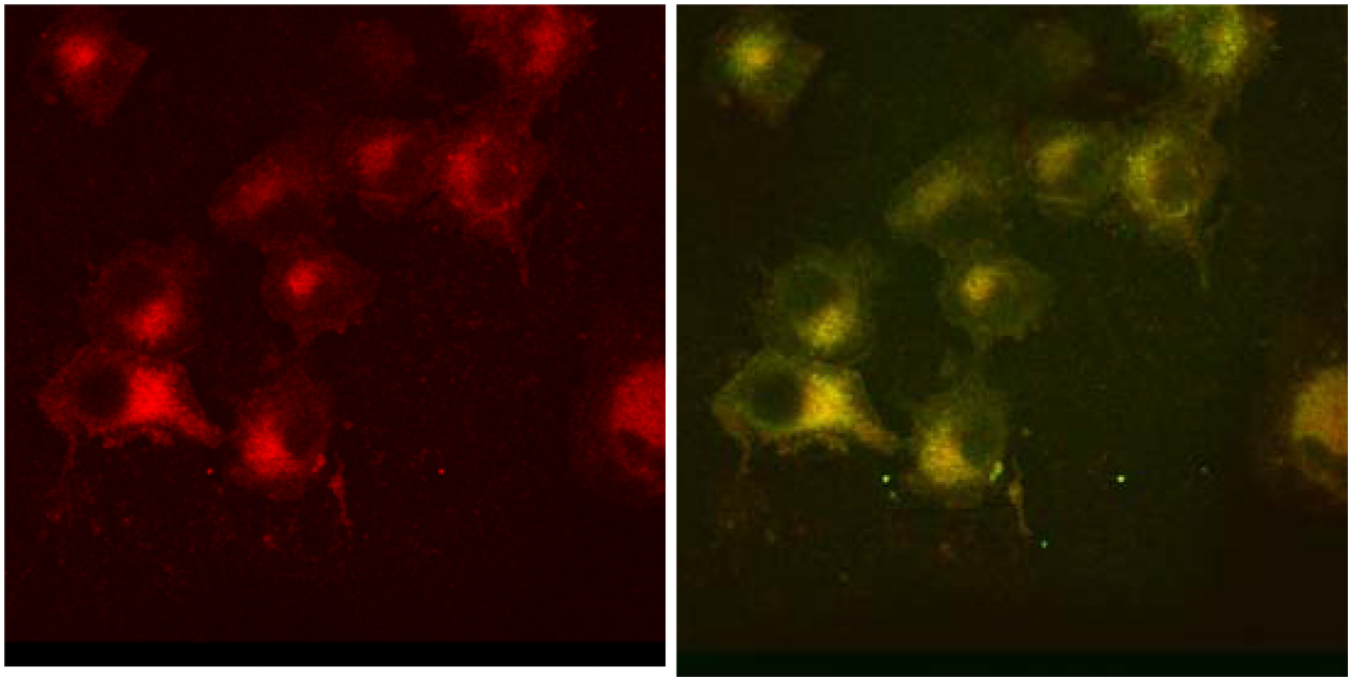

Figure 7.
Lung cancer cells treated with LS166 and costained with mitotracker green. Panel A shows the 780 nm channel alone, panel B shows the 488 nm and 780 nm panels merged. Yellow areas indicate co-localization. (Ye, et al., 2008))

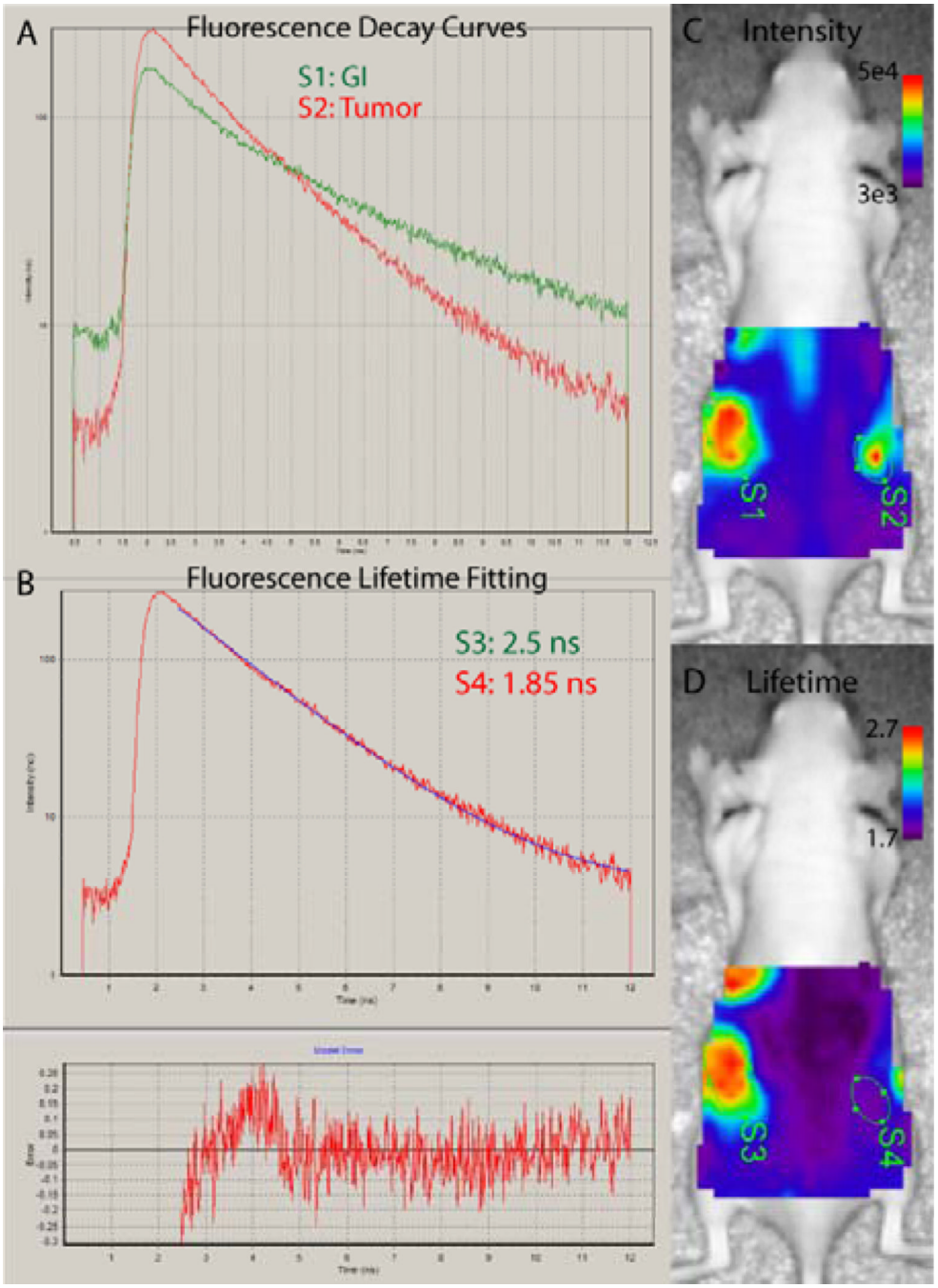

Figure 8.

Anticipated results from time-domain diffuse optical imaging. (A) fluorescence decay curves are collected for each measurement point in a raster scan of selected 2D region. (B) The fluorescence lifetime can be determined by fitting the tail of the decay curve. (C) Fluorescence intensity maps can be created by integration of fluorescence counts. Regions of interest are selected manually to determine average fluorescence intensity from dietary contents in the gastrointestinal (GI) tract (S1) or tumor (S2). (D) Fluorescence lifetime maps are created from fitting of the decay curves for each point. This map shows that the fluorescence from the GI (S3) can be distinguished from that of the fluorescent molecular probe in the tumor (S4) by differences in lifetime.